Journal of Welding Technology
P-ISSN: 2716-1471 | E-ISSN: 2716-0475
http://e-jurnal.pnl.ac.id/Welding_Technology

Analysis of SMAW welding parameters on the mechanical properties and microstructure of the ladder on dredger vessel at Perum Jasa Tirta 1

David Muhklison Hudiyanto*, Mujahid Wahyu, Ahmad Dzulfikri Halimi
Department of Mechanical Engineering, State Polytechnic of Malang, Indonesia
*Corresponding author: tkro1.29.muhklison@gmail.com

Article Processing Dates:
Received 2025-07-16
Accepted 2025-10-18
Available online 2025-12-31

Keywords:
Ladder vessel dredger
SS400
Welding current
Travel speed welding
Tensile test
Microstructure

Abstract

The ladder component on the dredger plays a crucial role in supporting vertical pressure or high hydrostatic forces during dredging operations, especially in water conditions with strong currents. In addition, it also supports cutting components and suction pumps, making the selection of materials and structural design essential to prevent failure. This study aims to analyze the structure of the ladder component that has been modified based on the welding method used. The research was conducted experimentally by varying welding parameters, including welding current and travel speed, to determine their effect on mechanical properties and microstructure. Welding was performed using E7018 electrodes with currents of 90 A, 100 A, and 110 A, and travel speeds of 5 cm/min, 7.5 cm/min, and 10 cm/min. Mechanical properties were evaluated through tensile testing (following ASTM E8 standards) using a testing machine with a maximum load capacity of 10 tons, and microstructure analysis was carried out by metallographic observation under an optical microscope at 100x magnification. The results show that increasing current and travel speed up to an optimal point can produce higher tensile strength, with the highest result of 399.67 MPa achieved using the welding parameters of 110 A and 10 cm/min travel speed. Moreover, increases in current and speed led to microstructural changes, showing a finer and more uniform grain distribution, especially in the HAZ and weld metal, which contributed to the improvement in mechanical properties. ANOVA test results indicated that the welding current, travel speed, and their interaction had a significant effect on tensile strength.

1. Introduction

A dredger vessel is heavy equipment operated by water resource management agencies, such as Perum Jasa Tirta I in Malang Indonesia, to mitigate sedimentation in river basins. One of the main structural components of a dredger vessel is the ladder, which functions as a connecting frame between the vessel hull and the cutter head. The ladder directs the cutter head toward the riverbed to fragment sediment, which is subsequently suctioned and transported to disposal areas on land. The required dredging depth varies depending on sedimentation conditions in each river basin [1][2].

At the Sengguruh Dam, one of the river basins managed by Perum Jasa Tirta I, sedimentation has increased significantly, reaching an average of 5,000,000 m³ annually, resulting in a continuous rise in dredging operations [3]. To address this issue, the Perum Jasa Tirta I workshop increased dredging capacity by modifying the ladder length from 10 m to 14 m to extend dredging reach [4][5]. This modification increased ladder weight and vertical hydrostatic loading during dredging operations, making proper alignment between material mechanical properties and welding parameters essential to prevent structural failure [6]. Previous ladder modifications were carried out without comprehensive material analysis, Welding Procedure Specifications (WPS), or post-weld mechanical testing. As a result, the structural reliability of the modified ladder remained uncertain and posed a potential risk of failure during operation [7][8]. Therefore, this study aims to investigate the effects of welding current and travel speed on the mechanical properties and microstructure of SMAW-welded SS400 steel used in dredger ladder components.

This experimental study varied welding current and travel speed parameters, both of which significantly influence mechanical properties. Previous studies have reported that these parameters strongly affect the mechanical properties and microstructure of SS400 steel [9][10]. Mechanical properties were evaluated using tensile testing to determine strength and fracture characteristics, while microstructural observations were conducted in the weld zones to identify optimal welding parameters for the material used [11][12].

2. Research methodology

This study employed an experimental method to evaluate the relationship between welding current and travel speed as independent variables and tensile strength and microstructure as dependent variables. Statistical and descriptive analyses were used to identify cause–effect relationships resulting from variations in welding parameters. Fig. 1-2. shows the ladder components of the dredger ship belonging to Perum Jasa Tirta 1 which was modified.

Fig. 1. *Modified Ladder Components*

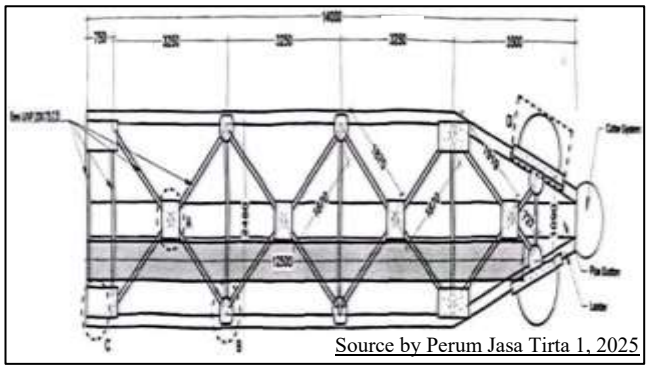

Fig. 2. *Ladder dredger vessel*

The research object was the ladder component of a dredger vessel owned by Perum Jasa Tirta I. The ladder was fabricated using IWF 300 structural steel with material specification JIS G 3101 SS400. This steel grade is widely used in construction projects due to its good strength, ductility, and formability characteristics [10].

The following mechanical properties of IWF 300 SS400 steel are listed in Table 1.

Table 1. Mechanical Properties Sructural steel 400

Type of testing	Properties	Test value
Tensile test	*Yield strength*	379 N/mm^2
	Tensile strength	480 N/mm^2
	Elongation	29 %
Bending test	180° R = 1.5 T	*Good*

Source by Perum Jasa Tirta 1, 2025

Overall, SS400 steel has a combination of good tensile strength, high ductility, and excellent formability, so that the characteristics of this steel are suitable for use in non-critical ship structural applications [13].

The study conducted re-welding with the same welding parameters as the ladder modification, but with varying welding current and speed to determine the significance of the changes in mechanical properties and microstructure. The following is a list of the materials and joints used in this study, as shown in the Fig. 3.

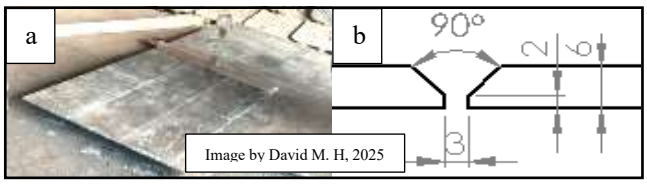

Fig. 3. (a) SS400 steel material, (b) Weld joint bevel dimensions

Fig. 3 (a) shows SS400 steel prepared by oxy-acetylene gas flame cutting and finishing using a hand grinder. Fig. (b) shows the dimensions of a welded joint with a 45° v-groove butt joint type.

Welding was performed using the Shielded Metal Arc Welding (SMAW) process with DCEP polarity and E7018 electrodes with a diameter of 3.2 mm. Welding currents of 90 A, 100 A, and 110 A were applied, combined with travel speeds of 5 cm/min, 7.5 cm/min, and 10 cm/min. Travel speed control was achieved using a stopwatch and marked welding paths to ensure consistency[14][15][16].

After welding, specimens were prepared for tensile testing and microstructural examination. Tensile test specimens followed the ASTM E8 standard using flat specimens with a thickness of 6 mm. Microstructural specimens were prepared through cutting, mounting, grinding, polishing, and etching before observation under an optical microscope at 100× magnification. Observations were conducted on three primary zones: base metal, heat-affected zone (HAZ), and weld metal [17]. The following are the shapes and dimensions of the test specimens based on the tests in this study shown in the Fig. 4.

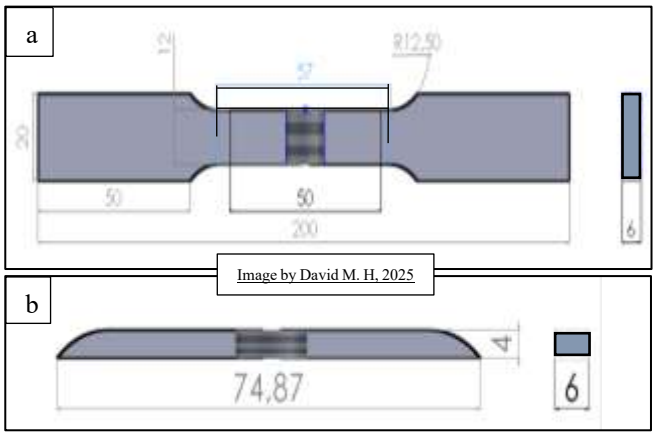

Fig. 4. (a) Dimensions of tensile test samples, (b) Dimensions of microstructure test samples

Fig. 4(a) shows the shape and dimensions of the tensile test specimen with ASTM E8 standard flat specimen with a thickness of 6 mm, has a narrowed neck so that the stress is concentrated in the middle of the specimen, so that the tensile test results are more accurate in showing the mechanical properties of the material, including yield strength, tensile strength, and elongation. In Fig. (b) shows the shape and dimensions of the micro test specimen taken from the remaining pieces of the tensile test specimen used for microstructure testing for further preparation stages in the form of cutting, mounting, grinding, polishing, and etching before being observed using an optical microscope.

3. Results and Discussion

The welding process was carried out in 3 layers (root pass, fill pass, and capping), each specimen showed consistent weld bead results according to the parameters used as shown in the Fig. 5.

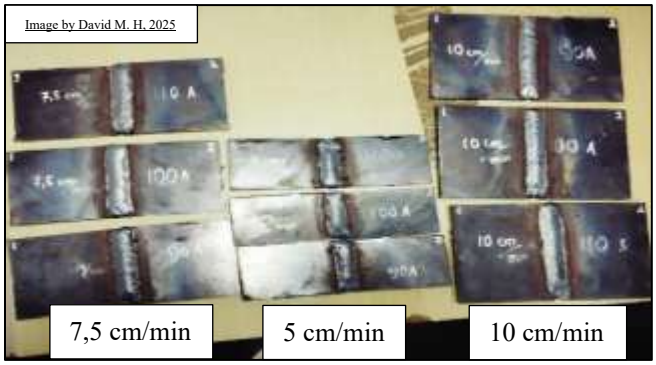

Fig. 5. Welding results

The welding results showed that all weld joints were formed successfully without any noticeable visual defects such as large porosity, undercuts, or incomplete fusion.

The welds were then subjected to tensile test specimens and microstructure tests, as shown in the Fig. 6.

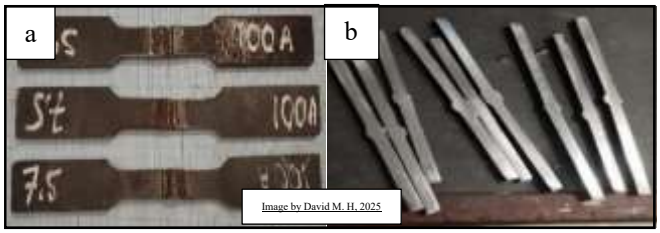

Fig. 6. Test specimen shape

Tensile test specimens were made in the amount of 27 samples because there were 3 replications in each welding variation and microstructure tests in the amount of 9 samples for each welding variation without repetition or replication. The tensile test results consist of visual types of fractures, load numbers that can be held and tensile strain numbers, while the microstructure test results consist of images of phase and grain shapes in 3 zones in each sample to be compared between parameter variations.

Tensile testing produces two types of fractures: fractures in the base metal zone and fractures in the heat-affected zone. The following shows the two fracture visuals in the tensile test, shown in the Fig. 7.

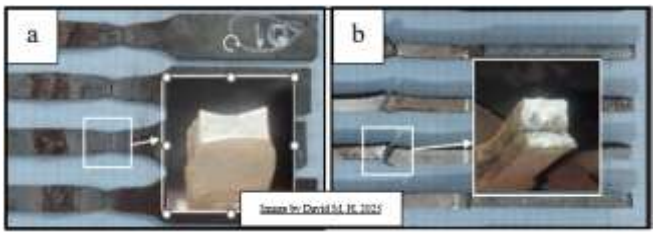

Fig. 7. Tensile test fracture results

Fig. 7(a) shows 19 specimens that broke in the parent metal, with visual results showing longitudinal strain fibers with necking in the parent metal. This indicates that the resulting welded joint is relatively strong against tensile loading [18]. As for image (b), 9 tensile test samples broke in the heat exposure zone (HAZ) with visual results showing weak points in the lower weld layer (root pass) that appear brittle and fragile, indicating that the lower weld layer (root) and the heat exposure zone have low strength [19].

The tensile test results obtained require conversion from the initial units of tensile load test results (kg) to (MPa) and length increase (mm) to (%) for correct reporting and comparison according to standards and engineering literature [20][21].

The following Table 2. shows the tensile test results obtained based on each combination of welding parameters, along with unit conversions.

Table 2. Tensile test results for welded joints

Current, (A)	Weld speed, (cm/min)	Replication	σ (MPa)	σ_y (MPa)	ε (%)
90	5	1	329,11	238	40,74
		2	321,45	224	39,42
		3	316,98	210	37,36
		Average	**322,51**	**224**	**39,17**
	7,5	1	314,02	244	34,18
		2	310,16	222	40,82
		3	302,88	246	36,14
		Average	**309,02**	**237**	**37,04**
	10	1	304,21	213	41,58
		2	303,95	203	40,54
		3	307,92	218	40,08
		Average	**305,36**	**211**	**40,73**
100	5	1	323,25	254	21,16
		2	239,33	200	13,58
		3	349,73	248	39,34
		Average	**304,10**	**234**	**24,69**
	7,5	1	353,65	233	37,36
		2	366,84	260	42,88
		3	302,51	214	21,54
		Average	**340,98**	**235**	**33,92**
	10	1	343,14	246	38,04
		2	339,79	242	38,32
		3	338,35	250	35,12
		Average	**340,42**	**246**	**37,16**
110	5	1	290,42	227	16,48
		2	311,35	201	16,20
		3	302,04	205	15,74
		Average	**301,27**	**211**	**16,14**
	7,5	1	369,53	260	42,88
		2	385,45	204	38,88
		3	382,85	202	28,94
		Average	**379,31**	**222**	**36,90**
	10	1	385,41	276	38,88
		2	383,85	278	43,56
		3	399,67	329	48,62
		Average	**389,64**	**231**	**43,68**

The tensile test results obtained show that the welding parameters (current and welding speed) have a significant effect on the mechanical properties (tensile stress, maximum stress, and material yield). High welding speed combined with high current produces the highest tensile strength value due to low heat input, resulting in faster cooling, but when compared with the tensile strength of SS400 material in the material certificate, the tensile test results of the welded joint experience a decrease in mechanical properties. So that the welding process can reduce tensile strength due to the presence of HAZ areas and weld metals that experience differences in microstructure, although there are still tensile strength values close to the original material. Several other external factors are an indication of a decrease in tensile strength caused by the treatment of materials from related industries, including the use of materials in a guerrilla manner, have been exposed to several less-controlled material preparation and storage processes [22][23][24].

The tensile test data obtained were then subjected to further statistical analysis using ANOVA to generate statistical data in show Fig. 8. The tensile stress and yield strength data were declared normally distributed and homogeneous because the P value was > 0.05, so it could be analyzed using parametric analysis (ANOVA). Meanwhile, the strain data were not declared normal because the P value was < 0.05, therefore a non-parametric Kruskal-Walis test was performed.

a) ANOVA test of tensile stress

Analysis of Variance

Source	DF	Adj SS	Adj MS	F-Value	P-Value
Ampere	2	9098	4548,9	8,53	0,002
Travel Speed	2	7277	3638,5	6,82	0,006
Ampere*Travel Speed	4	9945	2486,2	4,66	0,009
Error	18	9603	533,5		
Total	26	35923			

Model Summary

S	R-sq	R-sq(adj)	R-sq(pred)
23,0981	73,27%	61,39%	39,85%

Fig. 8. ANOVA statistical results on tensile stress

The ANOVA results show that the welding current/ampere, welding speed/travel speed and the interaction of the two have a P-Value less than the specified alpha value (P-Value < α) so that it is stated to have a significant influence on the mechanical properties of tensile strain with an R-sq value of 73.27% as shown in the Fig. 9.

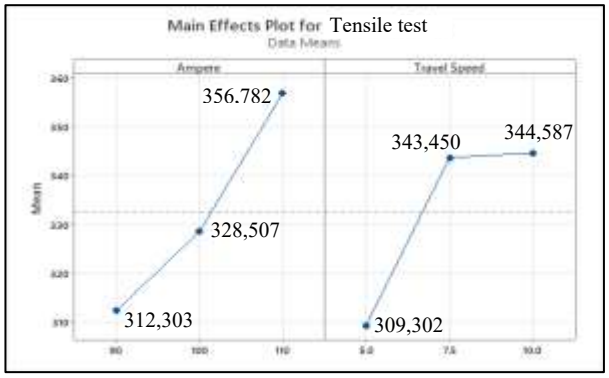

Fig. 9. Main effect plot of ampere and travel speed to tensile test

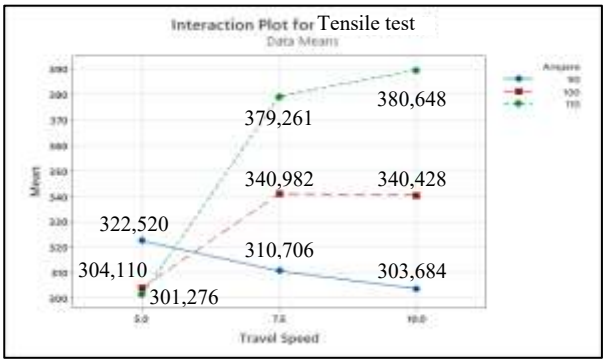

Fig. 10. Interaction plot ampere and travel speed to tensile test

Fig. 10 Main effect plot shows a significant increase in tensile stress as both current and welding speed increase. Fig. 10. Interaction plot shows that welding current has a more dominant influence than welding speed; the three lines are seen to be non-parallel (some are decreasing, some are stable, some are increasing), so there is an interaction effect between the two on tensile stress. The highest current (110 A) and medium (100 A) showed a significant increase in tensile stress as welding speed increased. Conversely, the lowest current (90 A) produced a tensile stress that tended to decrease as welding speed increased. Meanwhile, the medium current (100 A) showed a relatively stable trend with a slight increase at a speed of 7.5 mm/s. It can be seen that these three lines are non-parallel (some are decreasing) [16].

b) Non parametric test *Kruskal Walis* to tensile strain

Kruskal-Wallis Test: Tensile Strain versus weld current

Kruskal-Wallis Test on Regangan maksimum

Ampere	N	Median	Ave Rank	Z
90	9	40,08	16,9	1,36
100	9	37,36	11,2	-1,29
110	9	38,88	13,8	-0,08
Overall	27		14,0	

H = 2,34 DF = 2 P = 0,310
H = 2,35 DF = 2 P = 0,309 (adjusted for ties)

Fig. 11. Kruskal Wallis statistical results of welding current against tensile strain

Based on the results of the Kruskal Wallis non-parametric statistical analysis, the P-Value value for increasing or decreasing welding current against tensile strain was 0.309 > 0.05, so it was stated that there was no significant difference and had not shown a strong enough tendency towards maximum strain statistically [25].

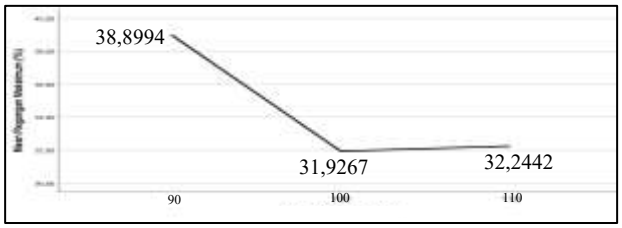

Fig. 12. *Individual Plot* welding current to tensile strain

Although the median and average rank (Ave rank) of 90 ampere has the highest median strain, this is not enough to be considered significant according to the Kruskal-Wallis test because it takes into account the entire distribution of data and its spread because in the individual plot it shows that increasing current also has an impact on reducing tensile strain [26].

Kruskal-Wallis Test: Tensile Strain versus Travel Speed

Kruskal-Wallis Test on Regangan maksimum

Travel Speed	N	Median	Ave Rank	Z
5,0	9	31,16	9,2	-2,24
7,5	9	37,36	14,3	0,15
10,0	9	40,08	18,5	2,08
Overall	27		14,0	

H = 6,25 DF = 2 P = 0,044
H = 6,25 DF = 2 P = 0,044 (adjusted for ties)

Fig. 13. Kruskal-Wallis statistical results of welding speed against tensile strain

Based on the results of the non-parametric statistical analysis of Kruskal Wallis, the P-Value was 0.044 <0.05, so there was a significant influence between the maximum strain on the welding speed parameter. The ave rank value showed that the higher the welding speed, the greater the maximum strain, this was shown that the speed of 5 cm/min had the lowest rank value and the speed of 10 cm/min showed the highest value, so that the increase in welding current had a significant effect on tensile strain and the increase in welding speed could increase tensile strain.

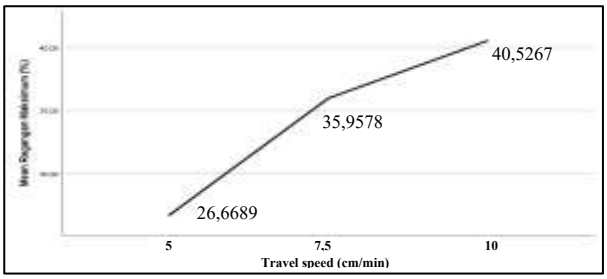

Fig. 14. Individual plot of welding speed against tensile strain.

The following interaction plot is displayed with ANOVA to show the trend of parameter combinations as additional data, although in fact the interaction significance test cannot be carried out because the method used is Kruskal–Wallis.

Tests of Between-Subjects Effects

Dependent Variable: Regangan Maksimum (%)

Source	Type III Sum of Squares	df	Mean Square	F	Sig.	Partial Eta Squared
Corrected Model	1793,638[a]	8	224,205	5,153	,002	,696
Intercept	31921,831	1	31921,831	733,631	,000	,976
KecepatanPengelasan	897,589	2	448,794	10,314	,001	,534
ArusPengelasan	286,109	2	143,054	3,288	,061	,269
KecepatanPengelasan * ArusPengelasan	609,941	4	152,485	3,504	,028	,438
Error	783,218	18	43,512			
Total	34498,687	27				
Corrected Total	2576,856	26				

a. R Squared = ,696 (Adjusted R Squared = ,561)

Fig. 15. Individual Plot of strain against welding speed.

The interaction between the current parameters and welding speed on tensile strain was analyzed in SPSS. The interaction showed a significant influence on maximum strain as shown by a sig value of 0.028 < 0.05 with an effect size (Partial Eta Squared) of 0.438 or 43.8%. This is still in the large category.

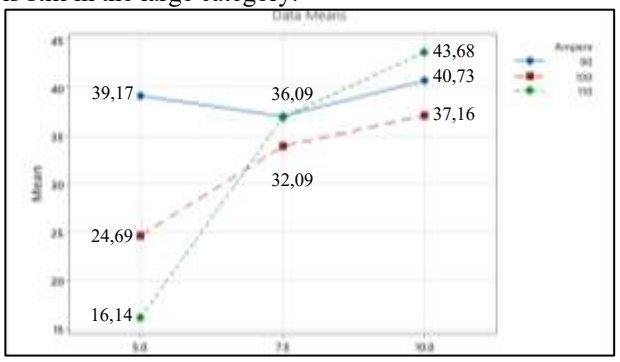

Fig. 16. Individual plot of strain against welding speed.

The interaction is demonstrated by the difference in the effect of welding speed on maximum strain, which depends on the welding current value. It can be seen that at speeds of 7.5 and 10 cm/min, the increase in maximum strain tends to be more stable.

c) ANOVA test of yield strength

```
Analysis of Variance

Source                 DF  Adj SS  Adj MS  F-Value  P-Value
  Ampere                2    1658   828,9     1,85    0,186
  Travel Speed          2    3574  1786,8     3,98    0,037
  Ampere*Travel Speed   4    9992  2497,9     5,56    0,004
Error                  18    8081   448,9
Total                  26   23304


Model Summary

      S    R-sq  R-sq(adj)  R-sq(pred)
21,1879  65,32%     49,91%      21,98%
```

Fig. 17. ANOVA results on yield strength.

Based on the results of the Two-way ANOVA factorial analysis, the welding speed shows a P value = 0.037, so it is considered to have a significant effect on the yield strength while the welding current shows a P value = 0.186. The results in the main effect plot Fig. show that both have increased, but at medium currents and speeds there is a significant difference.

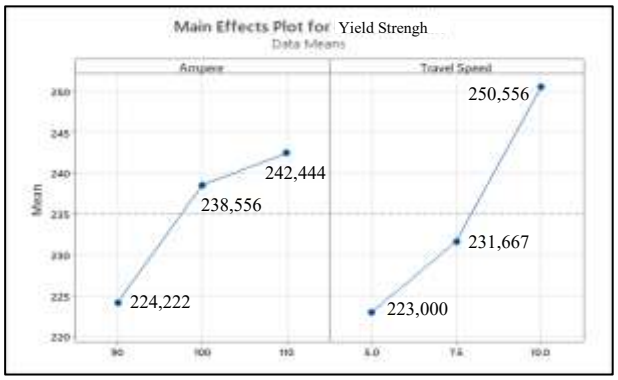

Fig. 18. Main effect plot of welding current and speed on yield strength.

The interaction between the two variables showed a P value of 0.004, indicating a significant interaction on yield strength. Although the current variation did not show a significant effect individually, its interaction with travel speed statistically affected the final results. The R-squared value of 65.32% indicates that the regression model was able to explain most of the data variation.

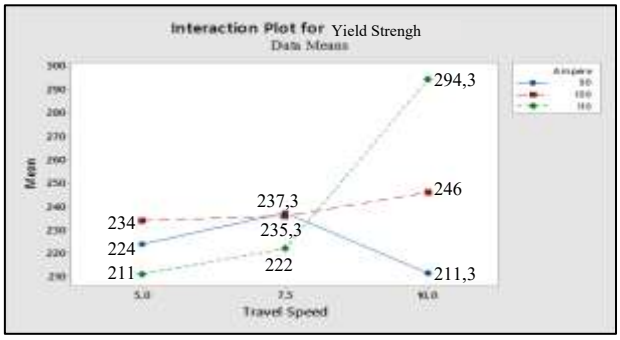

Fig. 19. Interaction Plot on yield strength.

The graph above shows that the current and welding speed parameters are not parallel and even intersect, indicating a significant interaction between the current and welding speed parameters. Welding speed parameters significantly affect the yield strength, and increasing the current parameter is more effective when combined with high welding speed parameters, so the two cannot be separated.

The microstructure testing was analyzed by observing the photos obtained using an optical microscope, with a magnification of 100x based on each zone, showing changes in the ferrite and pearlite phase grains in the heat exposure zone (HAZ) and the weld metal zone [27][28].

a) Microstructure of 90 A weld current and welding speed 5 cm/min

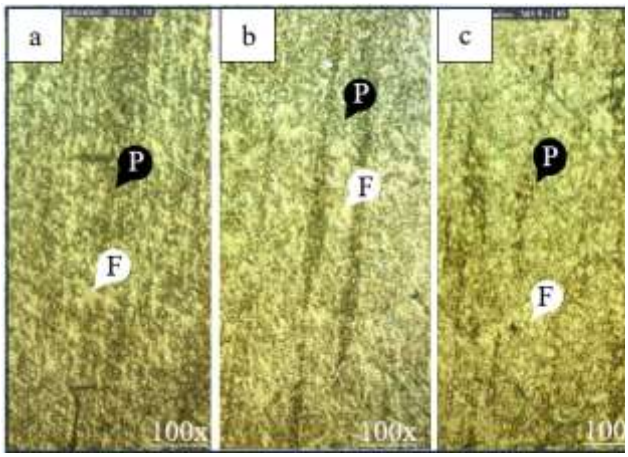

Fig. 20. Welding zone current 90 A with welding speed 5 cm/min.

Fig. 20 a) shows the microstructure of SS400 steel in its initial condition, where the metal surface is dominated by a fine pearlite phase and a ferrite phase that is evenly distributed with the grain size of both phases appearing fine and homogeneously distributed.

Fig. 20 b) shows the surface microstructure of the heat-exposed zone. Significant changes are seen with increasing grain size, both phases are coarser than the parent metal with an increasing proportion of ferrite. This zone undergoes phase transformation due to heating without melting, with the distribution of larger and coarser grains making the HAZ a mechanically weak zone, potentially reducing strength and toughness.

Fig. 20 c) shows the surface microstructure of the weld metal zone. Significant changes from the previous zone are seen, with coarser grains with a columnar orientation or grain reference indicating solidification of the weld fluid, dominated by ferrite forming an acicular or widmanstatten structure, and a little pearlite. This zone experiences total melting and re-solidification formed from slow cooling, which has the potential to reduce the tensile strength and toughness of the joint.

b) Microstructure of 90 A weld current and welding speed 7,5 cm/min

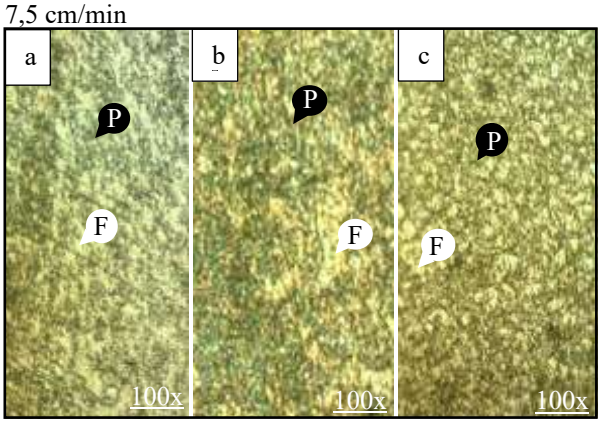

Fig. 21. Welding zone current 90 A with welding speed 7.5 cm/min.

Fig. 21 a) shows the microstructure of SS400 steel in its initial condition, where the metal surface is dominated by a fine pearlite phase and a ferrite phase that is evenly distributed with the grain size of both phases appearing fine and homogeneously distributed.

Fig. 21 b) shows the surface microstructure of the heat-exposed zone. Significant changes are seen with increasing grain size, with ferrite being unevenly distributed and tending to be coarse. This zone undergoes phase transformation due to heating without melting, with increasing grain size tending to reduce tensile strength and toughness.

Fig. 21 c) shows the surface microstructure of the weld metal zone. Significant changes from the previous zone are visible, with coarser grains with random grain orientation and clear grain boundaries dominated by ferrite and a little pearlite in an irregular shape. Faster cooling speeds of 7.5 cm/min result in a finer structure potentially having more stable mechanical properties, but the grains remain coarser than the HAZ or base metal.

c) Microstructure of 90 A weld current and welding speed 10 cm/min

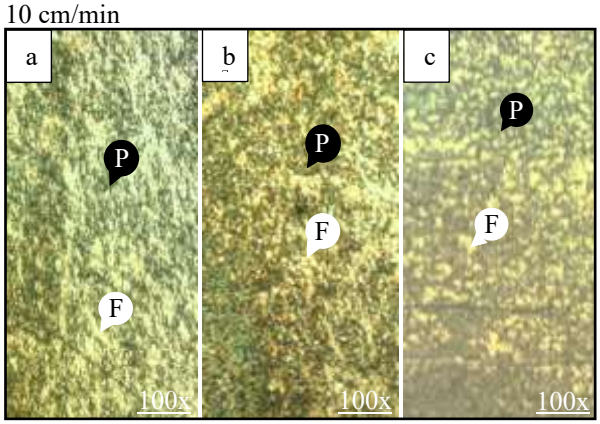

Fig. 22. Welding zone current 90 A with welding speed 10 cm/min.

Fig. 22 a) shows the microstructure of SS400 steel in its initial condition, where the metal surface is dominated by a fine pearlite phase and a ferrite phase that is evenly distributed with the grain size of both phases appearing fine and homogeneously distributed.

Fig. 22 b) shows the surface microstructure of the heat exposure zone. Grain growth is visible but not as large as at lower welding speeds, pearlite appears to be distributed less regularly with ferrite dominating. Because the relatively high welding speed results in a shorter heat exposure time, this limits the growth of ferrite grains in the HAZ, thus producing a finer and more stable structure that produces better mechanical resistance than at low welding speeds.

Fig. 22 c) shows the surface microstructure of the weld metal zone. Significant changes are seen from the previous zone, with finer grain appearance with a more random and dense grain distribution and grain boundaries that are more difficult to identify. High welding speeds accelerate the cooling process, resulting in rapid solidification of the molten metal. This results in denser ferrite and tends to inhibit the growth of coarse grains, thus improving mechanical properties, particularly tensile strength.

d) Microstructure of 100 A weld current and welding speed 5 cm/min

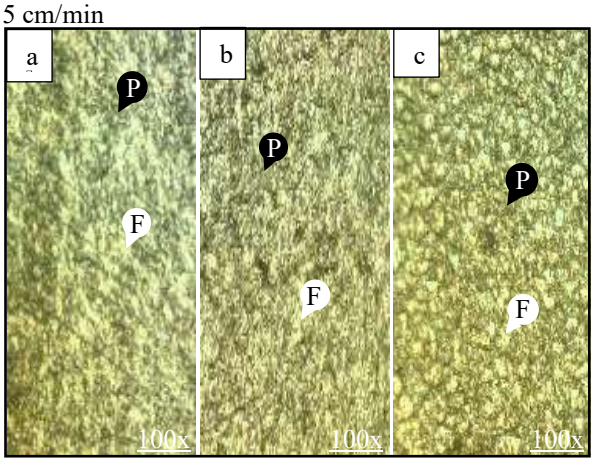

Fig. 23 Welding zone current 100 A and welding speed 5 cm/min.

Fig. 23 a) shows the microstructure of SS400 steel in its initial condition, where the metal surface is dominated by a fine pearlite phase and a ferrite phase that is evenly distributed with the grain size of both phases appearing fine and homogeneously distributed.

Fig. 23 b) shows the surface microstructure of the heat-exposed zone. Significant changes are seen with the ferrite grains enlarging and the pearlite starting to appear irregular. Both grain sizes are larger than the HAZ at higher welding speeds (7.5 or 10 cm/min) due to receiving heat for a long time, resulting in recrystallization and grain growth that can reduce toughness and tensile strength.

Fig. 23 c) shows the surface microstructure of the weld metal zone. Significant changes are seen, indicating a coarse and inhomogeneous structure, large ferrite grains and irregular grain shapes that tend to form columnar or dendritic. This is because the weld metal solidifies slowly, thus providing sufficient time for the growth of large and coarse ferrite grains.

Slow cooling causes the acicular ferrite structure to not form completely, thus possibly resulting in lower tensile strength. And this coarse structure is also more susceptible to weld defects such as porosity and microcracks.

e) Microstructure of 100 A weld current and welding speed 7,5 cm/min

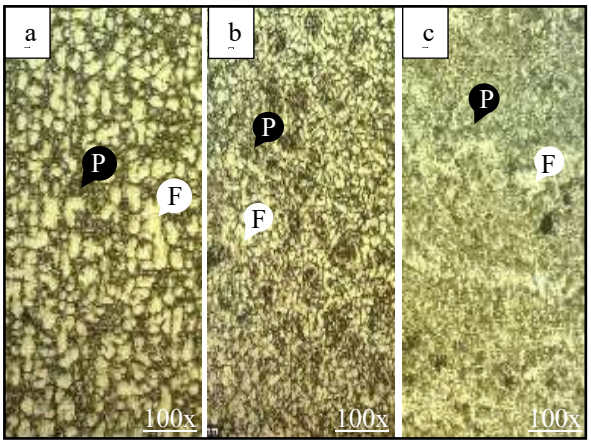

Fig. 24 Welding zone current 100 A and welding speed 7.5 cm/min

Fig. 24 a) shows the microstructure of SS400 steel in its initial condition, where the metal surface is dominated by a fine pearlite phase and a ferrite phase that is evenly distributed with the grain size of both phases appearing fine and homogeneously distributed.

Fig. 24 b) shows the surface microstructure of the heat exposure zone. Significant changes are seen with grain sizes increasing compared to the base metal. It appears that the growth of homogeneous ferrite grains with perlite begins to break down into smaller parts due to experiencing quite high heating but shorter than 5 cm/min welding, because the welding speed is higher (7.5 cm/min) so that grain growth still occurs but not as large as at low speeds. This structure tends to be more stable and stronger than the HAZ at a speed of 5 cm/min, but still risks reducing tensile strength when compared to the base metal.

Fig. 24 c) shows the surface microstructure of the weld metal zone. Significant changes are seen, indicating a finer structure compared to the welding speed of 5 cm/min with random grain orientation and a fairly even distribution of ferrite, the perlite begins to appear more homogeneous and less coarse. At a speed of 7.5 cm/min and a current of 100 A, the solidification process occurs at a moderate rate, producing an acicular ferrite structure and some columnar ferrite that is not too coarse. This indicates moderate cooling, resulting in better tensile strength and hardness than the slow speed combination (5 cm/min). The not too coarse and relatively smooth microstructure indicates a fairly optimal solidification condition.

f) Microstructure of 100 A weld current and welding speed 7,5 cm/min

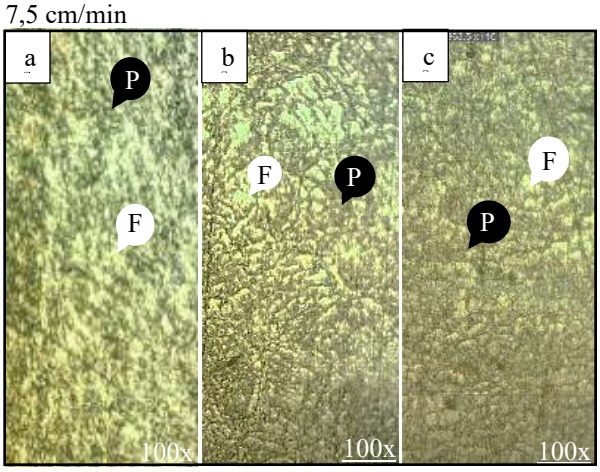

Fig. 25 Welding zone current 100 A and welding speed 10 cm/min

Fig. 25 a) shows the microstructure of SS400 steel in its initial condition, where the metal surface is dominated by a fine pearlite phase and a ferrite phase that is evenly distributed with the grain size of both phases appearing fine and homogeneously distributed.

Fig. 25 b) shows the surface microstructure of the heat-exposed zone. It is observed that there is little grain growth of ferrite and relatively small pearlite because the high welding speed (10 cm/min) with a current of 100 A results in a short heating time, as a result the recrystallization process and grain growth in the HAZ are limited, resulting in a finer and more stable structure compared to the HAZ at 5 and 7.5 cm/min. This is very positive because the HAZ is often a mechanical weak point, and a fine structure will increase the toughness and tensile strength in this zone.

Fig. 25 c) shows the surface microstructure of the weld metal zone. It appears to be a denser and smoother structure with a more even distribution of ferrite grains, with grain boundaries less pronounced than at slow welding speeds. This is because high welding speeds prevent the growth of large grains and produce a smooth and random acicular ferrite structure. Acicular ferrite is known to have high strength and good toughness, indicating that this microstructure offers superior weld joint quality and is more resistant to micro-defects such as porosity or segregation.

g) Microstructure of 110 A weld current and 5 cm/min welding speed

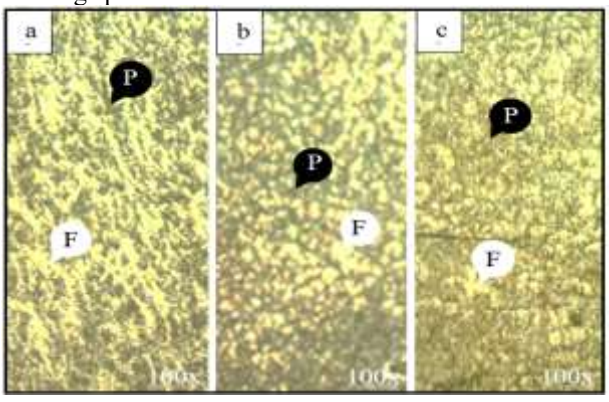

Fig. 26. Welding zone current 110 A and welding speed 5 cm

Fig. 26 a) shows the microstructure of SS400 steel in its initial condition, where the metal surface is dominated by a fine pearlite phase and a ferrite phase that is evenly distributed with the grain size of both phases appearing fine and homogeneously distributed.

Fig. 26 b) shows the surface microstructure of the heat-exposed zone. It shows very clear grain growth with larger ferrite and perlite grain sizes compared to other zones, and the grain distribution appears non-uniform, this is due to the combination of high current (110 A) and low welding speed (5 cm/min). The HAZ is exposed to heat for a longer duration which triggers recrystallization and excessive grain growth, this growth can cause a decrease in tensile strength and toughness because coarse grains tend to weaken the mechanical properties of steel in the HAZ zone.

Fig. 26 c) shows the surface microstructure of the weld metal zone. It shows a relatively coarse grain structure, non-uniform grain distribution, and indicates the presence of dominant ferrite with non-homogeneous pearlite distribution. This is due to the slow cooling process, causing grain growth in the weld metal to become larger and coarser. This structure can reduce the mechanical strength of the weld joint and increase the risk of micro-defects such as porosity or segregation.

h) Microstructure of 110 A weld current and 7,5 cm/min welding speed

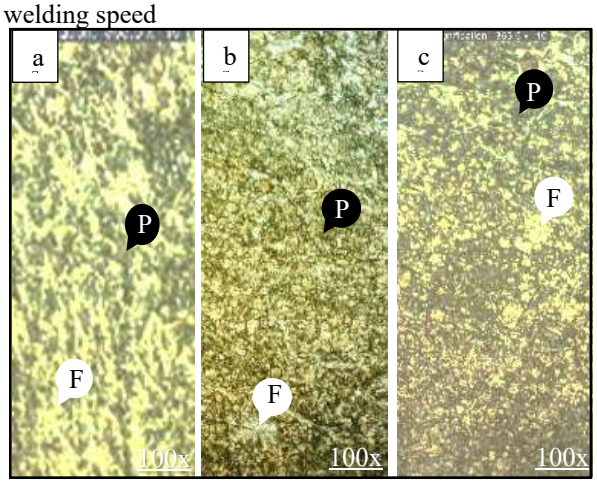

Fig. 27 Welding zone current 110 A and welding speed 7.5 cm/min

Fig. 27 a) shows the microstructure of SS400 steel in its initial condition, where the metal surface is dominated by a fine pearlite phase and a ferrite phase that is evenly distributed with the grain size of both phases appearing fine and homogeneously distributed.

Fig. 27 b) shows the surface microstructure of the heat-exposed zone. Larger ferrite and perlite grains are visible, with grain sizes showing some growth, but not as coarse as the 110 A – 5 cm/min variation. With a current of 110 A and a slightly higher speed (7.5 cm/min), the heating duration is slightly reduced, resulting in less grain growth than at the 5 cm/min speed. This structure has the potential to have slightly better tensile strength than the HAZ at slower speeds, but is still weaker than the base metal.

Fig. 27 c) shows the surface microstructure of the weld metal zone. A denser structure is seen compared to

the variation with a speed of 5 cm/min. The grain size is moderate and the distribution is relatively homogeneous, dominated by ferrite and a little pearlite. Because cooling takes place more quickly (due to the increase in welding speed), the weld metal structure formed tends to be smoother and more regular with a grain size that is not too large, this indicates an increase in the mechanical properties of tensile strength.

i) Microstructure of 110 A weld current and 10 cm/min welding speed

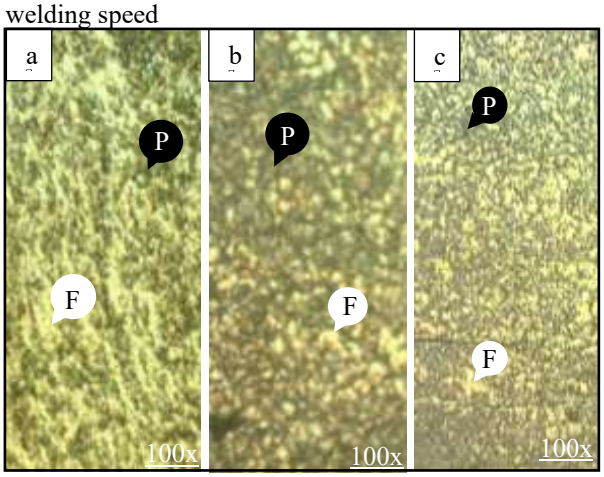

Fig. 28. Welding zone current 110 A and welding speed 10 cm/min

Fig. 28 a) shows the microstructure of SS400 steel in its initial condition, where the metal surface is dominated by a fine pearlite phase and a ferrite phase that is evenly distributed with the grain size of both phases appearing fine and homogeneously distributed.

Fig. 28 b) shows the surface microstructure of the heat exposure zone. It can be seen that ferrite and perlite grains experience moderate growth with a rather loose but not coarse grain distribution [28]. Not as bad as high current and slow speed conditions (e.g. 5 cm/minute). Because the welding speed is quite high (10 cm/minute) with a shorter heat exposure time, it suppresses excessive grain growth in the HAZ zone. This structure tends to provide a balance between strength and toughness.

Fig. 28 c) shows the surface microstructure of the weld metal zone. The structure is quite homogeneous with a relatively fine grain size slightly larger than the base metal, ferrite dominates with a little pearlite with a denser distribution compared to the weld results with slower speeds. At high currents with fast speeds resulting in relatively rapid cooling, this causes the formation of a finer microstructure in the weld area which improves the mechanical properties of tensile strength because the formation of columnar structures can be suppressed and random grains are more dominant.

4. Conclusion.

This study was conducted to analyze the effect of variations in welding current and speed on the mechanical properties and microstructure of SMAW welding results on SS400 steel used in the ladder components of the Perum Jasa Tirta 1 dredger ship. Based on the results of tensile tests, statistical analysis, and microstructure observations, the following conclusions were obtained:

1. Variations in welding current and speed have a significant effect on the mechanical properties of welded joints, including tensile strength, yield strength, and strain. The results of the ANOVA analysis show that current, welding speed, and the interaction between the two have a significant effect on tensile strength with a coefficient of determination (R^2) of 73.27%.
2. The combination of welding parameters of 110 A and a speed of 10 cm/min produced the highest tensile strength of 399.67 MPa with a maximum strain of 43.68%, indicating an optimal heat input balance.
3. Microstructural observations show that increasing the welding current and speed accelerates the cooling rate and produces finer and more uniform ferrite–perlite grains in the HAZ and weld metal. Conversely, the combination of high current and low speed causes coarser grain growth, thus reducing the mechanical strength.
4. Most of the specimens experienced fracture in the base metal, which indicates that the strength of the welded joint at optimum parameters approaches or exceeds the strength of the original material.
5. The results of this study emphasize the importance of selecting the right welding current and speed parameters, where the combination of 110 A and 10 cm/min is recommended as the optimal parameters for obtaining welded joints with high mechanical strength and smooth microstructure in structural applications of dredger ship ladder components.

Reference.

[1] H. Hariyono, "Analisis Kegagalan Struktur Ladder Pada Kapal Isap Produksi," *Wave J. Ilm. Teknol. Marit.*, vol. 16, no. 2, pp. 59–68, 2023, doi: 10.29122/jurnalwave.v16i2.5545.

[2] H. Hariyono, G. Sitepu, and M. Z. M. Alie, "Strength Analysis Due to the Elongation's Ladder of Cutter Suction Dredger Ship," *EPI Int. J. Eng.*, vol. 5, no. 1, pp. 1–9, 2022, doi: 10.25042/epi-ije.022022.01.

[3] S. Neumann, A. Kirichek, and A. van Hassent, "Agitat*s*., vol. 9, no. 2, pp. 218–224, 2024, doi: 10.12962/j25481479.v9i2.19417.

[6] A. Kagie, "Development of a numerical model for Cutter Suction Dredgers," 2018.

[7] R. S. Rachmat, L. Anggraini, W. Sihotang, and K. Ameyama, "Analysis of Welding Procedure Specifications for steel line pipe material," *Sinergi*, vol. 26, no. 3, p. 279, 2022, doi: 10.22441/sinergi.2022.3.002.

[8] P. Gangwar, "An Experimental Evaluation The Mechanical Properties , Microstructural Characteristics , And Weldability Of Grade 50 ASTM572 , GRADE A36 ASTM & GRADE 40c8 ASTM using Shielded Metal Arc Welding," vol. 12, no. 12, 2023.

[9] A. S. Mohruni and B. H. Kembaren, "Struktur Mikro Baja Karbon Rendah Dengan Elektroda E6013," *J. Rekayasa Mesin*, vol. 13, no. 1, pp. 1–8, 2013.

[10] H. K. Rahman and S. Sunyoto, "Pengaruh Arus SMAW Terhadap Kekuatan Tarik dan Impak Baja Konstruksi

IWF JIS G3101 SS400," *J. Din. Vokasional Tek. Mesin*, vol. 6, no. 1, pp. 35–45, 2021, doi: 10.21831/dinamika.v6i1.37070.

[11] M. Setiawan and D. R. Hartana, "Studi Pengaruh Arus Pengelasan Terhadap Sifat Fisis Dan Sifat Mekanis Sambungan Smaw Pada Baja Karbon Rendah," *Cendekia Mek.*, vol. 04, no. 02, pp. 102–113, 2023, [Online]. Available: https://journal.itny.ac.id/index.php/cendekia/article/view/4023

[12] F. Rozi, Abubakar, and Taufiq, "The effect of welding current on the mechanical properties of ST60 steel in the SMAW welding process," *J. Mech. Eng. Fabr.*, vol. 1, no. 1, pp. 20–24, 2024.

[13] J. Hasil *et al.*, "JURNAL TEKNIK PERKAPALAN Pada Sambungan Las Baja SS 400 Akibat Pengelasan Flux-Cored Arc Welding (FCAW) Dengan Variasi Suhu Normalizing," *J. Tek. Perkapalan*, vol. 7, no. 4, p. 323, 2019, [Online]. Available: https://ejournal3.undip.ac.id/index.php/naval

[14] M. Herranz, S. Rozas, and S. C. Balamili, "Sustainability assessment of shielded metal arc welding (SMAW) process Sustainability assessment of shielded metal arc welding (SMAW) process", doi: 10.1088/1757-899X/244/1/012001.

[15] H. Helanianto, E. Epriyandi, and H. Rahmadi, "Pengaruh Variasi Arus Pengelasan Smaw Terhadap Kekerasan Logam Induk Dan Logam Las," *Elem. J. Tek. Mesin*, vol. 7, no. 2, pp. 138–147, 2020, doi: 10.34128/je.v7i2.148.

[16] A. Sifa, L. Van Gunawan, Annifah, and Badruzzaman, "the Effect of Travel Speed and Electrical Current on Physical and Mechanical Properties of Cnc Mig Welded Low Carbon Steel Plate a36," *J. Teknol.*, vol. 87, no. 3, pp. 475–485, 2025, doi: 10.11113/jurnalteknologi.v87.21992.

[17] Husaini, N. Ali, J. K. Hamza, and S. E. Sofyan, "Effects of welding on the change of microstructure and mechanical properties of low carbon steel," *IOP Conf. Ser. Mater. Sci. Eng.*, vol. 523, no. 1, 2019, doi: 10.1088/1757-899X/523/1/012065.

[18] S. K. Gupta, A. P. Patil, R. C. Rathod, A. Gupta, H. Methani, and V. Tandon, "Cold Metal Transfer Welding of Ferritic and Austenitic Stainless Steel: Microstructural, Mechanical, and Electrochemical Studies," *J. Mater. Eng. Perform.*, vol. 33, no. 19, pp. 10663–10679, 2024, doi: 10.1007/s11665-024-09743-6.

[19] M. Aranđelović *et al.*, "Effects of Multiple Defects on Welded Joint Behaviour under the Uniaxial Tensile Loading: Fem and Experimental Approach," *Sustain.*, vol. 15, no. 1, 2023, doi: 10.3390/su15010761.

[20] T. Yu, "Tensile / Tension Test – Fundamentals –," 2017.

[21] T. O. Standard, A. American, and N. Standard, "Standard Test Methods for Tension Testing of Metallic Materials 1," 2013, doi: 10.1520/E0008.

[22] N. N. Vinh and D. H. Quan, "Grain boundary strengthening of microstructure phases in SS400 structural steel weld zone," *J. Sci. Technol. Civ. Eng. - HUCE*, vol. 17, no. 1, pp. 26–40, 2023, doi: 10.31814/stce.nuce2023-17(1)-03.

[23] H. Muqsalmina1, Syukran2, "Effect of temperature interpasses on mechanical properties welding process of SMAW SS400 carbon steel material," *J. Weld. Technol.*, vol. 1, no. 1, pp. 17–21, 2019.

[24] B. Ss and N. Mulyaningsih, "1 1* ," vol. 5, no. September, pp. 159–163, 2024.

[25] M. Al Fikri, I. Nugraha Gusniar, and D. V. Naubnome, "Effect of Welding Current (Smaw) on Tensile Strength and Microstructure of S45C Steel," *TRAKSI Maj. Ilm. Tek. Mesin* , vol. 22, no. 1, pp. 119–131, 2022, [Online]. Available: https://dx.doi.org/10.26714/traksi.22.1.2022.119-131

[26] S. P. Collins *et al.*, "Getting Started with the Kruskal-Wallis Test," *StatLab Assoc.*, pp. 167–186, 2021, [Online]. Available: https://library.virginia.edu/data/articles/getting-started-with-the-kruskal-wallis-test?utm_source=chatgpt.com

[27] W. Soedarmadji, "Pengaruh Pengelasan Shielded Metal Arc Welding (SMAW) pada Mild Steel S45C di Daerah HAZ dengan Pengujian Metalografi," *Mech. Manuf. Technol.*, vol. 1, no. 1, pp. 12–17, 2020, [Online]. Available: https://jurnal.yudharta.ac.id/v2/index.php/jmmt%0AVolume

[28] A. Halimi *et al.*, "Distribusi Ferrite dan Sifat Ketangguhan pada Pengaruh Media Quenching," vol. 6, no. 1, pp. 1–09, 2024, [Online]. Available: https://permadi.nusaputra.ac.id/index